Liquid Crystals
Publication details, including instructions for authors and subscription information:
http://www.informaworld.com/smpp/title~content=t713926090

Surface tensions of smectic liquid crystals

H. Schüring[a]; C. Thieme[a]; R. Stannarius[a]
[a] Universität Leipzig, Fakultät für Physik und Geowissenschaften, Linnéstr. 5, Leipzig 04103, Germany,

Online publication date: 06 August 2010

To cite this Article Schüring, H. , Thieme, C. and Stannarius, R.(2001) 'Surface tensions of smectic liquid crystals', Liquid Crystals, 28: 2, 241 — 252
To link to this Article: DOI: 10.1080/02678290010006270
URL: http://dx.doi.org/10.1080/02678290010006270

LIQUID CRYSTALS, 2001, VOL. 28, NO. 2, 241–252

Surface tensions of smectic liquid crystals

H. SCHÜRING, C. THIEME and R. STANNARIUS*
Universität Leipzig, Fakultät für Physik und Geowissenschaften, Linnéstr. 5, Leipzig 04103, Germany

(*Received 15 May 2000; in final form 28 June 2000; accepted 14 July 2000*)

We determine surface tensions σ of smectic liquid crystals from the curvature pressure of smectic films. A new technique is introduced for the comparison of surface tensions of different smectic materials. The method is based on the relation of curvatures of smectic films drawn on communicating vessels. The measurement of the temperature dependence of σ reveals anomalies in the vicinity of phase transitions to low temperature smectic modifications. This anomalous slope $d\sigma/dT$ can be related to the surface excess entropy of the material in the corresponding temperature range. The surface tension values determined for a number of mesogens fit well into the classification proposed by Mach *et al.*

1. Introduction

Smectic free-standing films (FSFs) have been studied extensively during the past two decades. They represent liquid crystalline systems of excellent macroscopic order. In particular, they prove very suitable for the determination of surface properties of liquid crystal materials. Because of the extraordinarily high surface to volume ratio, studies of surface ordering, surface induced phase transitions or surface tensions are conveniently performed in these systems. The study of the specific molecular interactions at interfaces is an attractive field of research today. Fundamental physical phenomena such as wetting and dewetting are intrinsically related to the action of surface tensions. A challenging question is the understanding of the relations between surface tension and molecular structure of fluids, its microscopic interpretation. Knowledge of this inter-relationship provides the basis for a controlled chemical modification of the surface properties of these materials. The study of smectic films is particularly promising for this task, because the films are characterized by highly ordered surface layers. The specific effects of individual molecular moieties on surface properties can be tested.

Another interesting feature is the investigation of the temperature characteristics of the surface tension. In ordinary isotropic liquids, the temperature dependence $d\sigma/dT$ is normally negative. Eötvös was the first to recognize that for many non-associating liquids the slope of $\sigma(T)$ can be scaled to a fundamental constant. However, an anomalous behaviour of that temperature dependence near the nematic–isotropic phase transition was found even in the early years of liquid crystal research [1, 2], and another anomaly at the nematic–smectic phase transition was also reported [3]. Of particular interest is the temperature dependence of σ in the context of thermally driven convection in thin films [4].

In this paper we present a detailed investigation of the surface tension for several smectic phases. In general, the temperature characteristics are similar to that of isotropic liquid phases, but anomalies are observed in the vicinity of phase transitions between certain smectic modifications. With the assumption of surface excess entropy contributions to the surface tension we are able to explain the experimental results.

Different methods for surface tension measurements of FSF have been developed in the past. Mach and co-workers [5–7] use a string tensiometer and record the deformation of a vertically suspended string under the action of surface tension forces when the string forms the border of a freely suspended smectic film. They have determined the surface tension σ for a large variety of smectic materials. Eberhardt and Meyer [8] have proposed a modified Wilhelmy balance. The device is sensitive to the force of a smectic FSF on a lateral barrier. The position of the barrier is detected with a laser beam and balanced by an electromagnet.

Another technique which exploits the analysis of the frequency spectrum of a film suspended over a circular hole in a solid substrate has been demonstrated by Miyano [9]. In addition, the straightforward Laplace–Young relation $p = 4\sigma/R$ between the inner excess pressure p and the radius R of a spherical bubble of smectic material has been used for the determination of the surface tension σ [10, 11]. Forces counteracting the

*Author for correspondence;
e-mail: stanni@anna.exphysik.uni-leipzig.de

Liquid Crystals ISSN 0267-8292 print/ISSN 1366-5855 online © 2001 Taylor & Francis Ltd
http://www.tandf.co.uk/journals
DOI: 10.1080/02678290010006270

deformation of the smectic film are created by the surface tension, the elastic deformation of the director field, the curvature elasticity of the membrane, and flexoelectric terms. For the rather large systems studied here, we can safely neglect all these influences except for the first one, the pressure generated by the surface tension according to equation (1). This method provides a direct and simple access to σ. The radius of a smectic bubble can be measured with high precision. If the bubble is sufficiently large, the relative error of the radius determination is smaller than 0.5%; the absolute scaling accuracy is somewhat larger. The measurement of the very small difference pressure is more problematic and requires a very sensitive pressure sensor. Since the pressure decreases with the inverse of the bubble radius, one has to make a compromise between accurate pressure and radius data. The precision of the surface tension data cannot be expected to be better than 1–2%. The competitive methods sketched above encounter approximately the same limits. A certain advantage of the bubble method is that systematical errors can be avoided easily.

The most comprehensive investigation of surface tensions of smectic fluids has been made by Mach *et al.* [7]. The study shows that the surface tensions of the mesogenic materials vary only in a rather small range. An important conclusion drawn by the authors is that the surface tensions of the investigated materials are basically determined by the terminating molecular subunits. The authors have provided a classification scheme which groups the investigated compounds in a few classes according to their chemical structure.

(1) Molecular cores disubstituted with hydroalkyl chains: these molecules are all characterized by surface tensions in a small range of $0.021 \pm 0.001\ \mathrm{N\,m^{-1}}$.
(2) Molecules with partially fluorinated alkyl substituents: the substitution of one or more hydrogens in the alkyl chains by fluorine reduces σ dramatically; surface tensions of the compounds in this class are distributed over a broad range below $0.019\ \mathrm{N\,m^{-1}}$, and in extreme cases σ is reduced to about $0.012\ \mathrm{N\,m^{-1}}$.
(3) Molecules with fully fluorinated chains: the surface tensions σ of materials with complete substitution of hydrogen by fluorine are grouped in a small range; the measured values of σ are $0.012 \pm 0.001\ \mathrm{N\,m^{-1}}$.
(4) Materials with hydroalkyl chains which have special packing properties, for example due to the existence of polar sub-groups in the molecule that favour the formation of bilayers. These materials provide larger surface tensions; they appear in the range from 0.023 to $0.027\ \mathrm{N\,m^{-1}}$.

Another key observation is that the surface tension of a smectic film is practically film thickness independent. If the tension changes with film thickness in very thin films of a few layers, this effect is below experimental resolution [7, 10].

If one is interested in studying how small modifications of the molecular structure influence σ, one usually deals with changes of only a few %. In particular, systematic investigations of homologous series require a high accuracy of the experiment. Since data on surface tensions which have to be compared are usually obtained from independent experiments, the experimental error doubles. The method proposed in this paper for an accurate comparison of surface tensions of two compounds is a modification of the bubble method. The basic idea is to use communicating vessels to support two smectic films; one film can be used as reference and therefore the pressure measurement can be eliminated. A direct relation between the radii of curvature of the deformed smectic membranes and their surface tensions can be established.

This paper is organized as follows. We describe the experimental set-up and sample preparation in the next section. The third section is subdivided into two parts; in the first the surface tensions of a numer of standard liquid crystal materials are given and compared with Mach's classification, and the second describes the experimental results for the temperature characteristics, interpreting the data qualitatively and quantitatively in the framework of the surface excess entropy model. Section 4 contains a general interpretation of the experimental results, comparing them with related experimental work by other authors, and discusses some more detailed aspects of the experiment. In the final section we give a short summary.

2. Sample preparation and experiment

The smectic materials studied in our experiments are: HOPDOB (4-hexyloxyphenyl 4-decyloxybenzoate), NOPB (4-nitrophenyl 4-octyloxybenzoate), 8CB (4-octyl-4′-cyanobiphenyl), 9OAB (4,4′-dinonyloxy-azoxybenzene), some Schiff's bases *n*O.*m* (4-*n*-alkyloxybenzylidene-4′-*n*-alkylaniline). DOBAMBC (4-decyloxybenzylidene-4′-amino-2-methylbutylcinnamate), and the commercial mixture FELIX-16/100 (Merck). The phase transitions are shown in figure 1.

A prerequisite for the experimental method described below is that stable free-standing smectic films of the materials exist. Therefore, we can perform the measurements over the temperature range where the samples are in the smectic A or smectic C/smectic C* phases. In the nematic range, in particular near the smectic phase transition, it is possible to obtain planar films but these films prove unsuitable for the bubble method; the

FELIX-016/100
X -20°C SmC* 72°C SmA 85°C N 94-90°C I

DOBAMBC
Cr 74.6°C (SmI* 62.0°C) SmC* 94.0°C SmA 117.0°C I

HOPDOB
(35.0 °C) Cr 62.5 °C E 38.0°C (B 44.5°C) SmC 77.5°C SmA 83.3°C N 88.9°C I

NPOB
Cr′ 47.5°C Cr 50.5°C SmA 61.4°C N 68.1°C I

8CB
Cr 21.5°C SmA 33.5°C N 40.5°C I

9OAB
Cr 75.5°C SmA 113.0°C N 121°C I

*n*O.*m*
n=4 *m*=4: Cr 9.0°C G 37.6°C SmB 44.8°C SmA 45.1°C N 74.3°C I
n=5 *m*=6: Cr 34.7°C G 37.4°C SmF 42.9°C SmB 51.4°C SmC 52.6°C SmA 61.3°C N 73.0 °C I
n=7 *m*=4: Cr 32.6°C G 63.9°C SmC 65.0°C SmA 75.0°C N 77.1°C I
n=7 *m*=6: Cr 38.5°C G 53.2°C SmB 65.4°C SmC 68.6°C SmA 81.1°C I
n=7 *m*=7: Cr 33.2°C G 48.0°C SmB 65.9°C SmC 70.0°C SmA 83.6°C N 84.4°C I
n=7 *m*=8: Cr 48.0°C G 53.0°C SmB 69.8°C SmC 70.3°C SmA 83.4°C I

Figure 1. Phase transition temperatures of the mesogenic materials investigated.

bubbles usually burst at the smectic–nematic transition. In the low temperature phases the films are very brittle. It is practically impossible to inflate films there, but bubbles can be transferred from SmA or SmC phases to some lower temperature smectic modifications. For the correct determination of surface tensions with our set-up, however, the dynamics of these films are too slow. This is discussed in detail below.

The general principles of the experiment have been described earlier [10]. For measurements of the absolute values and temperature dependence of surface tensions we have used a set-up which is basically equivalent to that shown in figure 2, but uses only one single capillary.

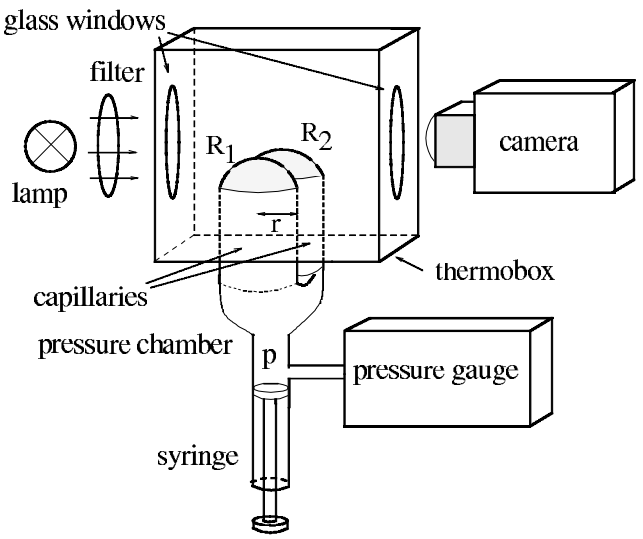

Figure 2. Experimental set-up for the generation and observation of the smectic membranes. We control the bubble volume by the air volume pumped into the chamber. The inner excess pressure of the chamber is measured with a commercial precision gauge. Capillary radii are between 1.5 and 5.5 mm.

The main part is the capillary tube mounted on an airtight pressure chamber. A free-standing smectic film is prepared on the capillary opening. The preparation technique, well known from soap films, is very simple but robust. A small amount of liquid crystal is placed on the face side of the glass capillary. Then the capillary opening is brought in contact with the face of a second tube of the same diameter. When the two tubes are drawn apart an initially almost cylindrical smectic film formed between the two cylinders takes the form of a catenoid which narrows rapidly when the capillaries are further separated [12–14]. At a critical distance between the tubes the catenoid collapses, and planar films are formed at the tube openings, the capillary can now be inserted in the set-up and connected to the closed chamber. After that we deflect the planar film to a bubble by controlling the volume of air in the chamber.

A copper box enclosing the upper end of the capillary with the smectic film ensures temperature stability and protects the film against air flow. Temperature is controlled with an accuracy of 0.2 K. The thermobox has two glass windows for optical observation. We illuminate the bubbles with parallel monochromatic light. The observation axis is horizontal, i.e. perpendicular to the capillary axes. The optical transmission images are recorded by means of a HAMAMATSU video camera and processed digitally in a computer. From the optical profiles of the bubbles, we can determine the membrane thickness of the smectic films [15]. The curvature pressure of the smectic film is counterbalanced by an excess pressure in the chamber. The equilibrium difference pressure between the chamber and the surrounding atmosphere in the stationary state is very small, and does not exceed 100 Pa. A sensitive capacitive pressure gauge is used to determine this pressure difference (absolute accuracy 2 Pa, relative accuracy about 0.1 Pa).

After a change of the air volume, the deflection of the films reaches a new static equilibrium very quickly (dynamic experiments show that the static deformation and pressure equilibrium are established within less than a second in SmA and SmC films); this is faster than the acquisition time of the pressure measurements (≈ 1 s). The static images are recorded, digitized with a resolution of $\approx 30\,\mu$m/pixel and the curvatures are determined by fitting the bubble images to a circular arc with image processing software. Within experimental resolution (as expected), no deviations of the bubble cross sections from a circular shape have been detected. The pressure data together with the film curvatures determined from the video images give the absolute surface tension with the help of equation (1).

In addition, we have used a slight modification of this standard set-up to compare surface tensions of different materials. Figure 2 sketches the modified experimental apparatus. The idea is to circumvent the pressure measurement as a possible error source when substances with slightly differing surface tensions are compared. Here we use two communicating capillaries to ensure that two films of different materials drawn on both openings experience the same lateral pressure.

After the preparation of free-standing films on each tube, we control the film deflection by injecting air into the pressure chamber. Because of the bistability of the system (discussed in the next paragraph) we inflate the films in this experiment only to approximate hemispheres. Initially, when the pressure in the chamber is equal to the external pressure, both films drawn on the capillaries are planar. The radii of curvature are $R_{1,2} = \infty$, where indices 1,2 refer to the two capillaries. When air is injected, the smectic films arch such that the curvature pressures of both films are equal to each other and to the chamber excess pressure. With increasing deflection of the film, the radius of curvature decreases, and simultaneously the excess pressure p in the communicating tubes increases. Figure 3 shows the theoretical dependence $p(h)$ where h is the height of the membrane deflection at its centre, with respect to the lateral meniscus. Let us assume first that the two films have equal surface tensions, then the film curvatures of both films will be identical. The maximum pressure $p_{max} = 4\sigma/r$ depends upon the capillary radius r, and is reached when the films form hemispheres. The half-spherical films rest approximately in the middle between the inner and the outer tube radii on the capillary glass wall. For the determination of the radii of curvature of the films, however, it is unimportant where exactly the bubble is supported.

When the film is deflected further, the radius of curvature increases again and the pressure reduces. A well known consequence of the curve shown in figure 3

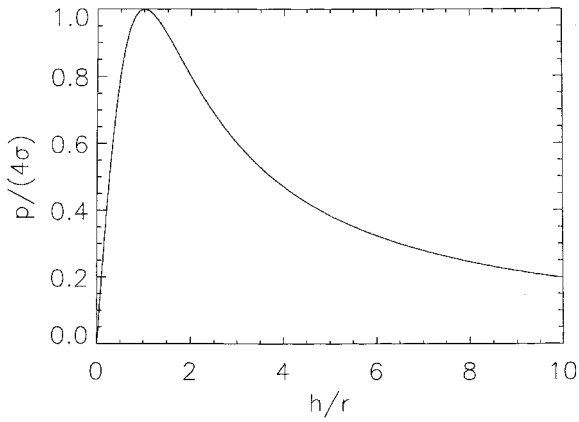

Figure 3. Dependence of the inner excess pressure p on the height of the film deflection $h = R \pm (R^2 - r^2)^{1/2}$ scaled with the capillary radius r.

is that there are always two different heights h of the film deflection which correspond to the same pressure $p < p_{max}$. If the air volume V injected is smaller than $V_c = (4/3)\pi r^3$, two identical sphere caps are formed. When more air is pressed into the chamber, two equilibrium states exist, a symmetric and an asymmetric one. The system always chooses the stable asymmetric solution

$$R = \left(\frac{3V}{4\pi}\right)^{1/3}$$

with $h = R + (R^2 - r^2)^{1/2}$ for one bubble, and $h = R - (R^2 - r^2)^{1/2}$ for the second (both caps can be added geometrically to give a complete sphere). Figure 4 (*a*) shows the stable symmetric solution in the case $V < V_c$ for two films produced with FELIX-16, and figure 4 (*b*) presents the same films in the stable asymmetric state at $V > V_c$. Since the reliability of the radius determination decreases when the deflection h of the films is small, we have performed our measurements preferably in the vicinity of $R \approx r$.

When the two surface tensions differ, e.g. $\sigma_1 > \sigma_2$, the film of larger surface tension σ_1 is always less deflected than the reference film and reaches its maximum deflection

$$h_{max} = r[\eta - (\eta^2 - 1)^{1/2}] \quad \text{with} \quad \eta = \frac{\sigma_1}{\sigma_2}$$

when the volume of air injected is

$$V = \frac{4\pi}{3}r^3 - \frac{\pi}{3}r^3(2\eta^2 + 1)(\eta^2 - 1)^{1/2}.$$

This method for comparison of surface tensions is particularly reliable when their difference is very small, i.e. when the comparison of two individual $p(r)$ curves becomes too inaccurate. If the surface tensions σ_1, σ_2 differ considerably, the determination of the curvature

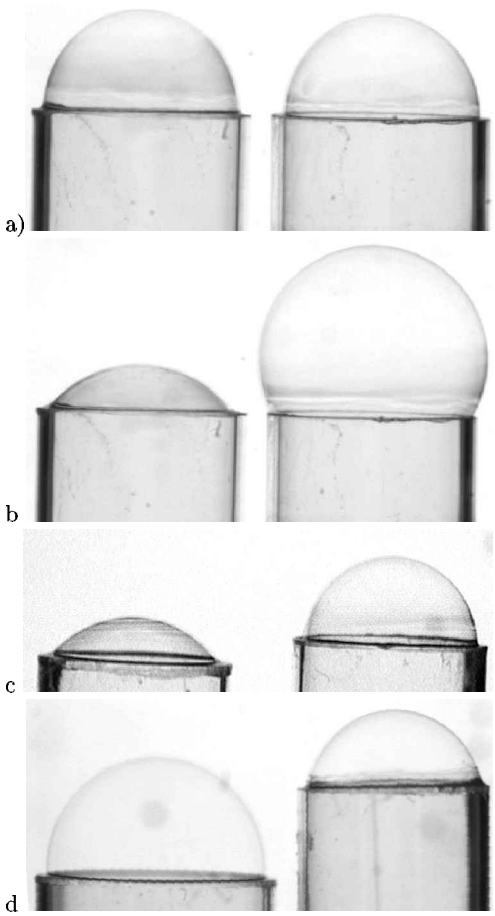

Figure 4. Smectic films on communicating vessels. The images have been contrast enhanced: (*a*) two identical films of FELIX-16, both (inner) tube diameters are $r = 3.85$ mm, $T = 22$°C. The radii of curvature $R_{1,2}$ as well as deflections $h_{1,2}$ of both films coincide; (*b*) after further inflation, the curvatures $R_{1,2}$ still coincide while the film deflections differ. (*c*) Two films with substantially different surface tensions, NPOB (left) and HOPDOB (right). (*d*) Same as in (*c*) but with two capillaries of different diameters $r_1 = 5.1$ mm, $r_2 = 4.05$ mm.

of the less deformed film is difficult with the desired accuracy. In those cases, we choose different radii r_1, r_2 for the two capillaries, where the ratio r_1/r_2 approximately matches the expected ratio of the surface tensions. Then, the comparison of the film curvatures can be performed with two approximate half-spheres and the determination of the radii is equally accurate for both films. This is demonstrated in figure 4 (*c*) showing the image of an NPOB film on the left and an HOPDOB film on the right capillary, both with the same radius *r*, and figure 4 (*d*) showing the analogous experiment where the capillary supported the NPOB film has a larger radius $r_1 = 1.26 r_2$.

A final remark concerns the influence of the film thickness on the σ measurements. It has been established in previous experiments that differences of the surface tension for thin and thick films of the same material are below the experimental resolution [7, 11]. Therefore, in most of our experiments the film thickness has not been considered critical. If not stated otherwise, the films investigated were between 20 and 50 layers thick. No particular attention has been given such that the films compared with the communicating capillary method had identical thickness. In some cases, the film thickness was not uniform over the whole sphere cap of the film. The film thickness may become important when in thin films the smectic phase sequences or transition temperatures change with respect to the bulk. This will be discussed in more detail in connection with the measurements for the Schiff's bases.

3. Results

3.1. *Comparison and classification of smectic materials*

We start with the temperature dependence of the surface tension for our reference substance FELIX-16 (figure 5) measured from the $p(R)$ curve of a single bubble. Since for these data, the measurement of the pressure difference was required, the absolute uncertainty of σ is about $\pm 2 \times 10^{-4}$ N m^{-1}. The broad range of the smectic A and C* phases allows comparisons with the surface tensions of a large number of different smectogens. The subsequent experiments were performed with the communicating capillary set-up where the reference film was FELIX-16 and the film on the second capillary consisted of one of the materials listed in the table. Our intention is to demonstrate the capabilities of the comparison method and moreover to test which of the compounds fit into Mach's classification. The quantity directly measured here is the ratio of the film curvatures $R_x/R_{\mathrm{FELIX}} = \sigma_x/\sigma_{\mathrm{FELIX}}$ given in the third column. By

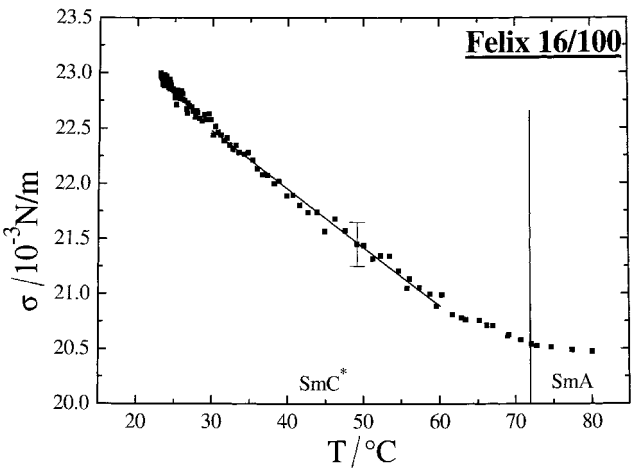

Figure 5. Surface tension $\sigma(T)$ of FELIX-16 obtained from the film curvature vs. pressure relation, equation (1) with the single bubble set-up.

Table 1. Ratio of the film curvatures of some of the investigated smectic liquid crystals and the reference material FELIX-16. This ratio is identical to the ratio of the surface tensions at the smectic/air interface.

x	T/°C	R_x /R_{FELIX}	σ_{FELIX} /10^{-3} N m^{-1}	σ_x /10^{-3} N m^{-1}
8CB	25.0	1.22	22.75	27.8
NPOB	53.0	1.23	21.3	26.2
HOPDOB	70.0	0.98	20.55	20.1
HOPDOB	52.0	0.96	21.35	20.4
HOPDOB	48.0	0.92	21.55	19.8
HOPDOB	46.0	0.91	21.65	19.7
9OAB	80.0	1.00	20.4	20.4

means of the reference surface tension of FELIX-16 (average extracted from figure 5) in column four, we have determined the absolute surface tensions given in the last column. Since the difference pressure does not influence the measured curvature ratios here, the surface tension ratios listed should be accurate to $\pm 1\%$. We note that the NPOB sample was the only material where the surface tension could not be exactly reproduced in subsequent experiments with different films; the measured data deviate by about 5%, and the given surface tension is the average of all measurements.

When the results are compared with the classification given by Mach *et al.* [7], the data are in full agreement with that model. Both HOPDOB and 9OAB belong to the class of fully hydrogenous chain molecules. The surface tensions of HOPDOB and all *n*OAB [16] are in the range predicted by the classification. We note, however, that the *n*OAB data are significantly lower than those reported for the alkyl chain substituted compounds *n*-AB [7]. The mixture FELIX-16 also falls into the same range; however, we cannot relate it to a molecular composition, as this has not been divulged by the manufacturers.

NPOB as a standard substance has been characterized extensively in the past. The polar nitro group of NPOB leads to a partial antiparallel short range order of the molecules [17]. NPOB, as well as 8CB, falls into the fourth class listed in the introduction. The comparatively high surface tension is a result of the packing properties of these materials. The validity of the classification given by Mach *et al.* [7] is therefore also confirmed for these two compounds. Measurements of the surface tensions within the *n*OAB homologous series indicate that the surface tensions of the compounds within the series (chain lengths 8, 9, 12 and 16) does not measurably depend upon the chain length [16].

The temperature dependence of the surface tension in the investigated compounds is in general very weak, only a few thousandths per Kelvin (cf. figure 5). Therefore the comparison of film curvatures at one temperature is sufficient to classify the material according to the above discussed scheme. For many materials, for example the *n*OAB homologues, the temperature dependence is rather similar to that of FELIX. However, there are striking exceptions, as one recognizes from the HOPDOB data in the table. We can therefore expect that the investigation of the temperature dependence of σ reveals interesting new effects. The next section is devoted to a detailed investigation of this temperature behaviour.

At this point it should be mentioned that before taking temperature curves, which is a time-consuming task that requires long term stability of the system, we have tested extensively the long term behaviour of the surface tension. It has been reported by several authors that the surface tensions of nematic liquid crystals determined with the droplet method are not constant in time, i.e. a freshly formed nematic surface shows a considerably different surface tension from a nematic surface exposed to air for hours or even days ([18] and refs. therein). The ratio of radius and inner excess pressure of a smectic DOBAMBC bubble has been recorded in our set-up over several days, and the variation of that ratio remained within the experimental uncertainty. *No* temporal trend has been observed in this experiment. We can state clearly that the surface tension immediately after the film is drawn (the establishment of equilibrium takes a few seconds) remains unchanged for days. This is obviously in contrast with the measurements for the nematic phase. We assume that in the nematic phase, the ordering processes of the molecules at the surface, e.g. the establishment of an equilibrium surface tilt and director field, is very slow (such very slow anchoring processes are also observed on solid substrates, see e.g. [19]).

3.2. *Temperature characteristics of surface tensions*

The simplest temperature characteristics of the surface tension, monotonous and almost linear, have been found in substances which possess long range SmA or SmC/SmC* phases and no other low temperature smectic phases, like the mixture FELIX-16. The surface tension of FELIX-16 slightly decreases with increasing temperature over the whole temperature range of the smectic A and C* phases (figure 5), a linear fit in first approximation from 30 to 60°C yields the slope $\mathrm{d}\sigma/\mathrm{d}T = -5.1 \times 10^{-5}$ N m^{-1} K^{-1}. The surface tension changes by slightly more than 10% over the temperature range studied in the smectic A and C* phases of the sample.

This corresponds qualitatively and also quantitatively to the behaviour of conventional isotropic liquids. The Eötvös rule predicts that for non-associated liquids the normalized surface tensions σ_{M} obey a common

temperature dependence

$$\sigma_M = k_M (T_K - T)$$

where T_K is a temperature near the critical temperature of the liquid, k_M is a universal constant equal to 2.1×10^{-7} N m K^{-1} and $\sigma_M = \sigma A_{mol}$ is a 'molar' surface tension given by the product of σ and the reference area $A_{mol} = V_{mol}^{2/3}$ derived from the molar volume V_{mol}. One can interpret σ_M as the surface energy per molecule at the surface, multiplied by the constant $N_A^{2/3}$ where N_A is the Avogadro number.

If we assume a molecular mass of about 450 and a density of 10^3 kg m^{-3} for the smectic mixture (di-substituted two-kernal molecules), which gives $A_{mol} = 5.9 \times 10^{-3}$ m^2, we obtain a value of $k_M = -\mathrm{d}\sigma/\mathrm{d}T \times A_{mol} = 3 \times 10^{-7}$ N m K^{-1}. It has the correct order of magnitude as predicted by the rule of Eötvös. Of course, in the ordered smectic phases the area $V_{mol}^{2/3}$ is not an ideal reference quantity since it supposes spatial isotropy. For the prolate shaped molecules in the investigated calamitic smectic, this area per molecule at the surface has to be corrected to lower values, bringing k_M down to the value characteristic for isotropic phases.

We notice a slight deviation of the slope in the vicinity of the (bulk) SmC* to SmA transition. This deviation is rather small, but systematic. However, we have found this effect with such clarity only in the FELIX-16 mixture. We consider two possible contributions to explain this behaviour. The first one is related to the fact that the surface tension in an anisotropic material is, strictly, a tensor property [20–22]. With our experimental method, we always measure only a certain component of this tensor property, along the smectic layer normal. In tilted phases it need not even be a principal axis of this tensor. If we suppose that the surface tension is larger for a surface which is normal to the director (i.e. to the average orientation of the molecular long axes) than for a tilted orientation, the change in the tilt angle towards the SmC*–SmA transition could explain the observed deviations from the linear $\sigma(T)$ curve. Another contribution could originate from a possible surface excess entropy near the phase transition, but we consider this contribution at the SmA–SmC* transition to be orders of magnitude smaller than the experimental uncertainty, as the following measurements and considerations will show.

The next material investigated in this study, the standard ferroelectric smectic material DOBAMBC, exhibits a phase transition from SmC* to a hexatic SmI* phase. The $\sigma(T)$ dependence of DOBAMBC is shown in figure 6. Two independent sets with different bubbles (denoted by solid squares and open circles, respectively) are shown. The plot reveals a rather linear temperature characteristic of the surface tension, with no significant peculiarities at the SmC*–SmI* transition. The slope

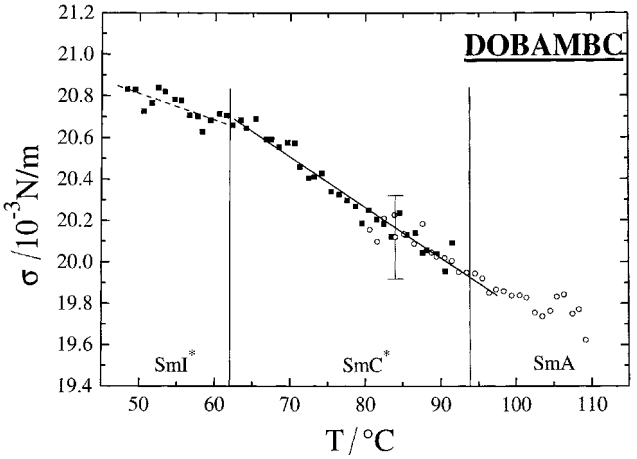

Figure 6. Surface tension $\sigma(T)$ of DOBAMBC obtained by the single bubble method.

$\mathrm{d}\sigma/\mathrm{d}T$ in SmC* is slightly smaller than for FELIX-16, and a linear fit between 65°C and 95°C yields approximately -2.4×10^{-5} N m^{-1} K^{-1}. This value is still in satisfactory agreement with the isotropic liquid model. And again, the small but systematic deviation of the slope $\mathrm{d}\sigma/\mathrm{d}T$ (more gentle at temperatures near the transition to SmA) seems to be indicated. Also, the slope of σ in the SmI* phase differs slightly from that in SmC*.

In general, we have found the same 'normal' behaviour, the negative temperature slope of σ, in all smectogens which exhibit only SmA and SmC/SmC* phases. This holds in particular for the *n*OAB homologous series [16]. In 8CB and NPOB the phase ranges are too narrow to allow a quantitative determination of the temperature coefficient, but the trend $\mathrm{d}\sigma/\mathrm{d}T < 0$ is clearly observed.

The temperature characteristics of σ near a SmC–B (cryst) transition have been studied in the material HOPDOB. We have acknowledged already in the table that the ratio of surface tensions between HOPDOB and FELIX-16 undergoes a dramatic change above the SmC–B transition. Figure 7 shows the surface tension data from $p(R)$ measurements of single bubbles of HOPDOB. At high temperatures, one finds a rather linear behaviour; $\sigma(T)$ decays monotonously with increasing temperature as in FELIX-16, but the slope is significantly smaller than for FELIX-16 (approximately -10^{-5} N m^{-1} K^{-1}). However, the $p(R)$ curve from which the surface tension was derived has a pronounced bend around 50°C, and the temperature slope of the σ values obtained changes its sign. This is a remarkable behaviour, since HOPDOB is not known to have a phase transition at 50°C. HOPDOB exhibits a transition into a monotropic B phase [23] with a bulk transition temperature of 44°C. We have confirmed that the abnormal temperature dependence is found in films up to thicknesses > 200 nm

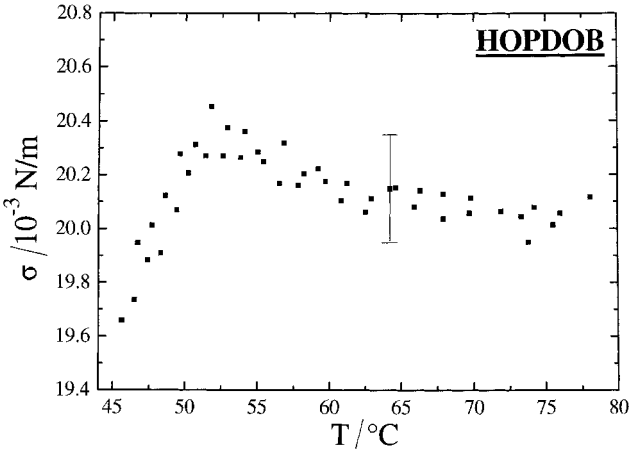

Figure 7. Surface tension $\sigma(T)$ of HOPDOB determined by the single bubble method. Note the change of the temperature characteristics of σ near 50°C in the pretransitional range of the B phase (see text).

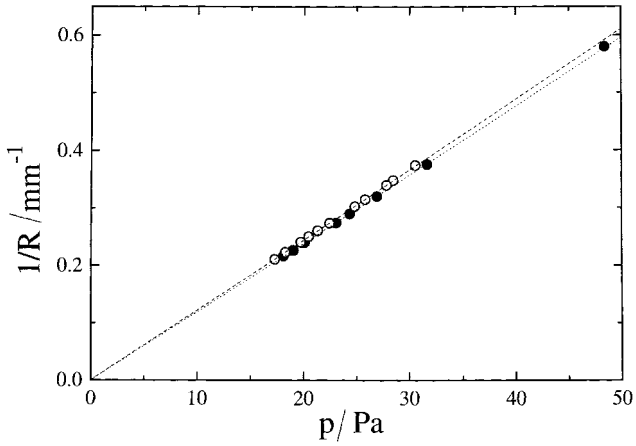

Figure 8. Plot of the inverse radius of curvature $1/R$ of a smectic bubble vs. the difference pressure p for HOPDOB at 54°C (solid) and 46°C (open). The straight lines symbolize the linear fits with slopes $1/(4\sigma)$, dotted line for 54°C, dashed line for 46°C. The Laplace–Young relation obviously holds at both temperatures. The lower surface tension belongs to the lower temperature (cf. also the table).

where we can exclude that the phase transition in the free standing smectic film is measurably shifted with respect to the bulk phase.

The prerequisite for our measurements is of course the validity of equation (1). If the fluidity in the smectic layers is lost and a lattice is formed, the $p(R)$ curve no longer reflects the surface tension. Therefore we have checked carefully that the film is still fluid. The HOPDOB bubbles can still be inflated and deflated in the pretransitional range to the B phase. The viscosity increases considerably when the phase transition is approached, and it takes several seconds until a constant inner pressure is established after a volume change in the bubble. However, no hysteresis was observed, i.e. the same pressure is found independent of whether a certain radius of curvature is approached from below or above. Figure 8 shows the plot of $1/R$ as a function of the difference pressure at 46°C (open symbols), together with the linear fit with slope $(4\sigma)^{-1}$ (dashed line). The solid symbols represent data measured at 54°C, together with the corresponding linear fit (dotted line). It is obvious that relation (1) is well fulfilled at both temperatures, but the surface tension is smaller at the lower temperature. Both data sets have been obtained with the same bubble; systematic errors are therefore excluded. At ≈45°C, a phase transition occurred in the smectic materials (obviously to CrB) and the bubble burst. We have not been able to cool freely suspended HOPDOB bubbles below that temperature.

The slope $d\sigma/dT \approx 11 \times 10^{-5}$ N m^{-1} K^{-1} is positive in a 5 K temperature range; a crossover in the temperature characteristics is found at 50°C. This anomalous slope is in agreement with the measured ratios $\sigma_{HOPDOB}/\sigma_{FELIX}$ from the table, which change by more than 5% in the temperature range from about 50 to 45°C. This anomalous behaviour has been confirmed by Veum *et al.* [24] from the vibration spectra of free standing films of the same material. The observed crossover is not related to a bulk phase transition temperature. However, we can interpret the anomaly by assuming a surface transition to the B phase. A higher ordered surface layer leads to an excess surface entropy s which is related to σ by [25]

$$\frac{d\sigma}{dT} = -s.$$

An increase of the film surface area leads to a transport of molecules from the less ordered bulk into the higher ordered surface layer. The amount of excess entropy per surface is thus approximately 11×10^{-5} J m^{-2} K^{-1}. We compare that quantity with the B–SmC transition enthalpy $\Delta H \approx 5$ kJ mol^{-1} [26–28] (literature data differ by about 10% which is not essential here). A monomolecular smectic B layer at the surface would give the excess entropy per area

$$s = \frac{\Delta H \rho d}{T_{BC} M_{mol}}$$

where d is the thickness of the SmB layer, T_{BC} is the phase transition temperature, ρ is the density ($\approx 10^3$ kg m^{-3}) and M_{mol} is the molar mass of 454 g mol^{-1}. Insertion of these data and an assumed thickness $d = 3$ nm gives a value of 10^{-4} J m^{-2} K^{-1}. If we compare this value with the temperature dependence of σ, we find that the increase of surface tension with temperature can be consistently explained by an approximately monomolecular smectic B surface layer on the smectic C film which is formed 5 K above the bulk transition.

We have tried to confirm this interpretation by studying other substances with transitions to lower temperature smectic modifications. The members of the *n*O.*m* homologous series provide a rich variety of smectic phase sequences. Figures 9 (*a–d*) depict the temperature dependence of the measured quantity $pR/4$ for six homologues of this series. The quantity $pR/4$ is representative for the surface tension as long as the experiment yields equilibrium quantities. This is the case in the smectic A and smectic C phases where the film dynamics are fast; the bubble radius is always in equilibrium with the inner excess pressure. We have marked these data, which are equivalent to σ, by solid squares or open circles in the figures. The solid squares in each figure represent a data set obtained with one and the same bubble, while open circles denote a second independent experiment, usually performed with a bubble of different film thickness.

In all homologues, we observe a positive slope of $\sigma(T)$ above the low temperature phases. The order of magnitude of $d\sigma/dT$ is the same as for HOPDOB (with the exception of 4O.4, see below). The transition enthalpies from SmC to SmB or G, respectively are known from the

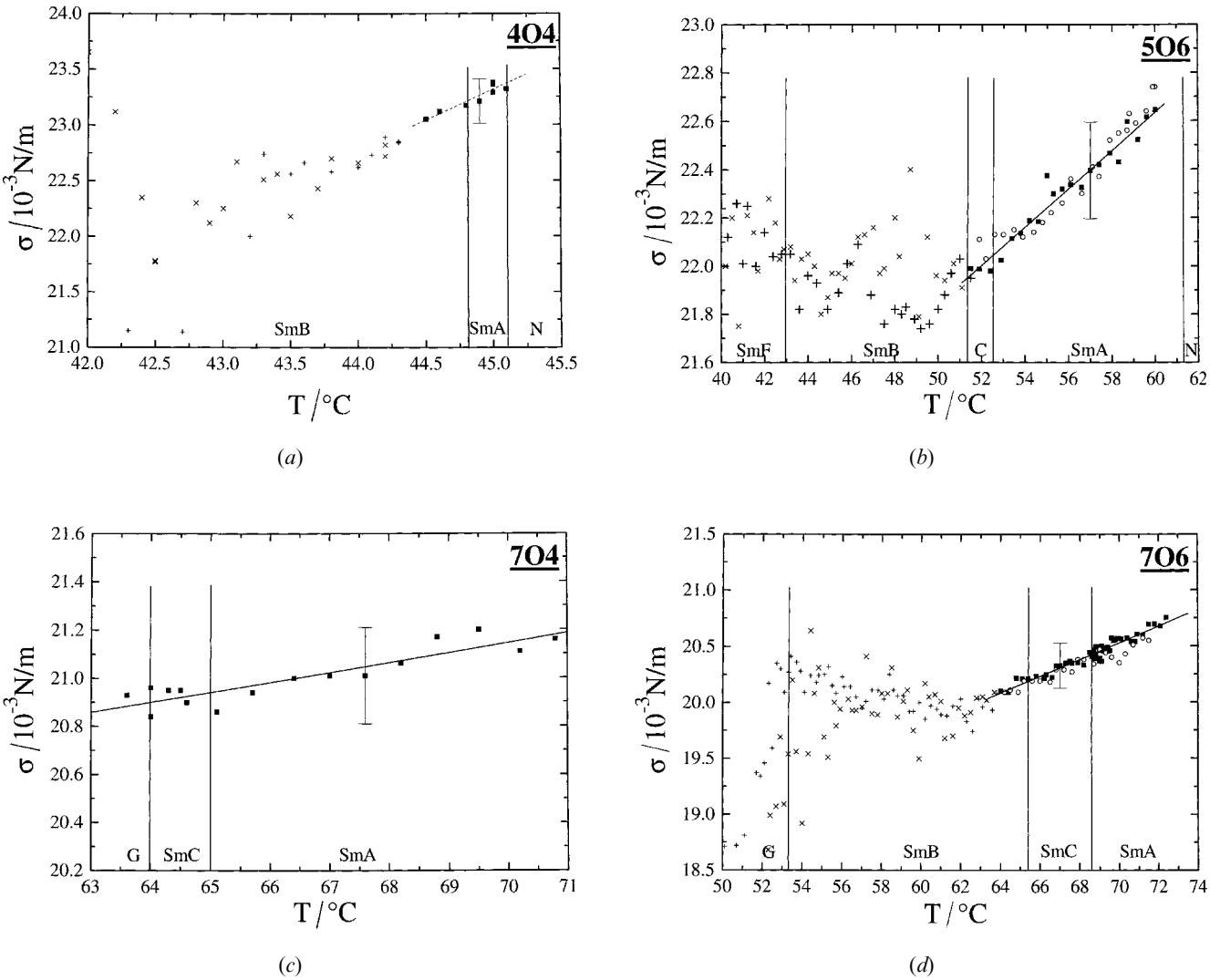

Figure 9. Surface tension measurements for Schiff's bases *n*O.m compounds. Solid squares denote σ (measured in one experimental run), open symbols denote a second independent experiment with the same material. Solid lines are linear fits to these data with the slopes given below. Crosses and plus signs symbolize the value of $pR/4$ at temperatures where the bubbles due to high viscosity do not reach an equilibrium pressure. (*a*). 4O.4: slope $d\sigma/dT \approx 5 \times 10^{-4}$ N m^{-1} K^{-1} (see text); (*b*) 5O.6: slope 7.9×10^{-5} N m^{-1} K^{-1} (squares $d = 22$ nm, ○ $d = 44$ nm); (*c*) 7O.4: slope 4.1×10^{-5} N m^{-1} K^{-1} ($d = 51$ nm); (*d*) 7O.6: slope 7.4×10^{-5} N m^{-1} K^{-1} (squares $d = 400$ nm, ○ $d = 180$ nm); for 7O.7 and 7O.8 the corresponding slopes of σ are 3.3×10^{-5} and 5.6×10^{-5} N m^{-1} K^{-1}.

literature [29]. For example, the 5O.6 homologue has a transition enthalpy of $\Delta H \approx 2.5\,\mathrm{kJ\,mol^{-1}}$ [30–32, 29] and with $M_{mol} = 351\,\mathrm{g\,mol^{-1}}$, $T_{BC} = 324\,\mathrm{K}$, $\rho \approx 10^3\,\mathrm{kg\,m^{-3}}$ we obtain an entropy change per volume

$$\Delta S = \frac{\Delta H}{T_{BC}} \frac{\rho}{M_{mol}} \approx 2.2 \times 10^4\,\mathrm{J\,m^3\,K}.$$

Again, this is in agreement with an excess surface entropy of $7.9 \times 10^{-5}\,\mathrm{J\,m^{-2}\,K^{-1}}$ when a smectic layer thickness of about 3.6 nm is assumed. For the other homologues, the results are rather similar. However, a systematic correlation between ΔH [29] and $\mathrm{d}\sigma/\mathrm{d}T$ cannot be detected.

So in the same way as for HOPDOB, we conclude that the existence of an ordered layer at the film surface leads to the anomalous behaviour of the surface tension vs. temperature. In contrast to HOPDOB, we have not observed an upper limit of this anomalous range, meaning that the ordered surface layers must exist across the whole range of the SmA/SmC phases. The short homologue 4O.4 has probably a much larger temperature dependence of σ, with positive slope. However, the observable temperature range is very narrow in this material and we consider the result only qualitatively correct. The linear fit curve is certainly not quantitatively representative.

A remarkable difference to HOPDOB is found when the material is cooled to the low temperature region. On the Schiff's bases, the bubbles survive the bulk phase transition to higher ordered smectic phases. The pressure vs. radius curves can still be recorded. The crosses and plus symbols in the images of figure 9 reflect the corresponding $pR/4$ data. The quantity $pR/4$ is not stationary, but rather the inner excess pressure fluctuates considerably at a given bubble radius. Therefore, the pressure data do not represent equilibrium values and we do not consider this measurement to reflect the surface tension of the materials. This is discussed in detail in the next section. However, if we average over these fluctuations, we can probably still get at least a rough estimate of the surface tension. When the sample temperature fluctuates around some given temperature, the $p(R)$ data will fluctuate around an average value determined by the surface tension. The general trend, seen for example in the 5O.6 data, seems to indicate that the slope $\mathrm{d}\sigma/\mathrm{d}T > 0$ is not continued at low temperatures. We suggest the following straightforward explanation: when the transition into the higher ordered phase has occurred in the bulk material, the surface excess entropy vanishes. However, the uncertainty of the σ-determination in that range is too large in our set-up, and some refined experiment has to be designed to allow clear quantitative statements about the temperature curve of σ here.

4. Discussion

The application of equation (1) is justified when the bubble responds to all temperature changes of the gas content by a corresponding radius change. Then, the equilibrium radius and pressure values can be used to determine the surface tension by equating the inner excess pressure to the curvature pressure of the film. What happens, however, if the film is too viscous to follow small volume changes of the gas enclosed by the bubble? Such volume changes occur as a consequence of thermal expansion of the air. It is realistic to assume that we can keep the temperature in the bubble constant to 0.03 K. According to the ideal gas equation, the product of bubble volume V and absolute inner pressure P is $PV \propto T$. Consequently the product PV changes by 10^{-4} following the temperature changes in the set-up, even when T fluctuates by only 0.03 K. This can be achieved in two ways. Either the dynamics of the smectic are fast compared with the temperature changes; then the smectic film shrinks or expands accordingly, the bubble radius performing small fluctuations of the order of only 3×10^{-5} following the temperature fluctuations. In this case, the system can reach and maintain the equilibrium pressure at a given bubble radius, the inner excess pressure remains stationary and equation (1) yields σ. This is the behaviour observed in the SmA and SmC/SmC* phases and also in DOBAMBC below the bulk SmC*–SmI* transition. The small radius fluctuations are not observable in our optical set-up.

On the other hand, if the film is too viscous to change the bubble volume fast enough, the temperature variation will mainly lead to a pressure fluctuation of the order of 10^{-4}. This corresponds to a change of the inner excess pressure p of the order of 10 Pa. The slower the response of the film to the air temperature changes, the larger will be the observed pressure fluctuations, and this is exactly what is observed in the experiments. It is obvious that in the experimental data, the fluctuations of pR (which essentially reflect pressure changes) increase with decreasing temperature, i.e. with higher viscosities of the films. We have not studied the dynamics quantitatively, since it is difficult to detect the tiny temperature fluctuations in the bubble without great experimental effort, but dynamic experiments in these low temperature phases should be an interesting subject for further investigations.

Another question is of course whether the films are in the same phases as the bulk material. This must generally be denied. It is known that the phase transitions in thin films can be remarkably shifted with respect to the bulk values, and moreover the phase sequences can be changed. We assume that the material of the inner film layers in the investigated Schiff's bases is not in a crystalline smectic (B or G) state, but probably remains

in a hexagonal (hexatic) smectic phase. Of course, if the film material is not in the same phase as the bulk (the meniscus, which serves as a reservoir for the smectic film) then the experiment strictly measures a film tension which consists of the contribution of the surface transition and an additional contribution from the entropy difference between material in the bulk and within the inner layers of the film. This should be considered in a more detailed theoretical analysis of the results presented here.

We can now apply the concept of excess surface entropy to the results of the DOBAMBC measurements. In DOBAMBC there is no reversal of the $d\sigma/dT$ slope above the SmC*–SmI* transition. The corresponding transition enthalpy ΔH of DOBAMBC is $\approx 1.6\,kJ\,mol^{-1}$ [33]. This value is roughly of the same order of magnitude as that for the SmC–SmB transitions in the Schiff's bases. With the molecular weight $477.7\,g\,mol^{-1}$ and density comparable to the *n*O.*m* homologues, one would expect a similar influence on the surface excess entropy if an ordered surface layer existed in DOBAMBC. The conclusion from the experiment is that the SmI* phase in this material obviously does not form a higher ordered surface layer.

5. Summary

We can summarize the results of this paper as follows: a new straightforward method has been developed to compare surface tensions at the liquid crystal–air interface of smectic mesogens. The ratios of surface tensions are determined from the ratios of the curvatures of free standing films. The method is particularly accurate for the study of small surface tension differences and relative changes of surface tension. Second, we have presented the first report on systematic surface tension measurements with the self-supporting smectic bubble method.

These two methods have been applied to study the dependence of surface tension upon molecular properties and the temperature characteristics of σ. The ratios of surface tension for a number of standard smectic materials have been determined and compared with the predictions of Mach's classification. The substances fit into that classification without exception. The materials investigated in this study can be classified into two groups. For the molecules with fully hydrogeneous alkyl chains, the surface tensions are in the range between 0.020 and $0.023\,N\,m^{-1}$. This is in accordance with the microscopic interpretation of the surface tensions given in [7]. The two substances with only one alkyl chain and a polar group at the opposite end of the molecules have surface tensions between 0.026 and $0.028\,N\,m^{-1}$ which is also in accordance with that classification.

The surface tensions of a number of smectic compounds with characteristic phase sequences have been determined as a function of temperature. We have compared the experimental results with the behaviour of simple isotropic liquids and predictions of a model which takes into account surface excess entropies.

For the commercial mixture FELIX-16, the temperature slope is negative and almost linear over a large temperature range with $d\sigma/dT \approx -5.1 \times 10^{-5}\,N\,m^{-1}\,K^{-1}$, and the behaviour can be explained qualitatively with the standard rule for non-associating liquids. To obtain a satisfactory quantitative agreement, one needs to introduce corrections for the anisotropic orientation of the molecules in the smectic phase. A comparable behaviour to that in this mixture has been found in DOBAMBC, with $d\sigma/dT \approx -2.4 \times 10^{-5}\,N\,m^{-1}\,K^{-1}$. In both materials, a small but systematic deviation towards a more gentle slope is observed near the transition from the tilted SmC* into the SmA phase. This can be explained qualitatively as a consequence of the tensor character of the surface tension in liquid crystalline phases.

The temperature dependence in NPOB and 8CB (within the relatively narrow smectic A phases) is comparable to FELIX-16. In general, a negative slope $d\sigma/dT$ has been found in all substances which do not exhibit higher ordered smectic modifications at lower temperatures. In the phenyl benzoate HOPDOB, at high temperatures the slope is only about $-1 \times 10^{-5}\,N\,m^{-1}\,K^{-1}$, but still negative. However, a significant exception is observed in this material in the smectic C phase within a 5 degree pre-transitional range to the low temperature B phase. The slope $d\sigma/dT \approx 11 \times 10^{-5}\,N\,m^{-1}\,K^{-1}$ becomes positive in that range, a crossover in the temperature characteristics is found at 50°C. This observation can be explained by the formation of a monomolecular smectic B surface layer on the smectic C film at about 5 K above the bulk transition. Such surface transitions have been reported in a number of studies in the past [34–38].

The same anomalous behaviour has been found in the SmA and SmC phases of all investigated homologues of the alkyloxybenzylidene-alkylaniline series (Schiff's bases *n*O.*m*). These materials are characterized by a rich polymorphism and transitions from SmA/SmC to low temperature SmB/G phases. The temperature slope is positive within the whole SmA/SmC range. A single layer of higher ordered molecules at the film surfaces persisting throughout the SmA/SmC temperature ranges can explain this anomaly, similar to that in HOPDOB. In the low temperature phases, our method does not provide reliable surface tension data.

The authors acknowledge financial support by the DFG within SFB 294. We are indebted to Thomas John for programming the image processing software and to C. Bahr for making manuscript [38] available prior to publication.

References

[1] Jaeger, F. M., 1917, *Z. anorg. allg. Chem.*, **101,** 1.
[2] Ferguson, A., and Kennedy, S. J., 1938, *Phil. Mag.*, **26,** 41.
[3] Krishnaswamy, S., and Shashidar, R., 1977, *Mol. Cryst. liq. Cryst.*, **38,** 353.
[4] Godfrey, M. I., and van Winkle, D. H., 1996, *Phys. Rev. E*, **54,** 3752.
[5] Stoebe, T., Mach, P., and Huang, C. C., 1994, *Phys. Rev. E*, **49,** R3587.
[6] Mach, P., Grantz, S., Debe, D. A., Stoebe, T., and Huang, C. C., 1995, *J. Phys. II Fr.*, **5,** 217.
[7] Mach, P., Huang, C. C., Stoebe, T., Wedell, E. D., Nguyen, T., De Jeu, W. H., Guittard, F., Naciri, J. Shashidar, R., Clark, N., Jiang, I. M., Kao, F. J., Liu, H., and Nohira H., 1998, *Langmuir*, **14,** 4330.
[8] Eberhardt, M., and Meyer, R. B., 1996, *Rev. sci. Instrum.*, **67,** 2846.
[9] Miyano, K., 1982, *Phys. Rev. A*, **26,** 1820.
[10] Stannarius, R., and Cramer, C., 1997, *Liq. Cryst.*, **23,** 371.
[11] Stannarius, R., and Cramer, C., 1998, *Europhys. Lett.*, **42,** 43.
[12] Maclennan, J., Decher, G., and Sohling, U., 1991, *Appl. Phys. Lett.*, **59,** 917.
[13] Chikina, I. V., Limodin, N., Langlois, A., Brazovskaja, M., Even, C., and Pieranski, P., 1998, *Eur. Phys. J.*, **B3,** 189.
[14] Ben Amar, M., da Silva, P. P., Limodin, N., Langlois, A., Brazovskaja, M., Even, C., Chikina, I. V., and Pieranski, P., 1998, *Eur. Phys. J.*, **B3,** 197.
[15] Stannarius, R., Cramer, C., and Schüring, H., 1999, *Mol. Cryst. liq. Cryst.*, **329,** 1035.
[16] Thieme, C., unpublished results.
[17] Ernst, S., Churjusova, T., Sokolova, E., Wiegeleben, A., Hansei, A., and Demus, D., 1994, *Cryst. Res. Technol.*, **29,** 297.
[18] Song, B., 1994, PhD thesis, TU, Berlin, Germany.
[19] Barberi, R., Dozov, I., Giocondo, M., Iovane, M., Martinot-Lagarde, P., Stonescu, D., Tonchev, S., and Tsonev, L. V., 1998, *Euro. Phys. J.*, **B6,** 83.
[20] Yokoyama, H., Kobayashi, S., and Kamei, H., 1984, *Mol. Cryst. liq. Cryst.*, **107,** 311.
[21] McMullen, W. E., and Moore, B. G., 1991, *Mol. Cryst. liq. Cryst.*, **198,** 107.
[22] Papenfuss, C., 1995, PhD thesis, TU, Berlin, Germany.
[23] Petrova, M., and Simova, P., 1986, *Cryst. Res. Technol.*, **21,** 959.
[24] Veum, M., Mach, P., Crowell, P. A., and Huang, C. C., 2000, *Phys. Rev. E*, **61,** R2192.
[25] Huang, C. C., 1998, in *Handbook of Liquid Crystals* (Heidelberg: Wiley-VCH), p. 441.
[26] Shashidar, H. D. K. R., 1981, *Mol. Cryst. liq. Cryst.*, **64,** 217.
[27] Demus, D., Pohl, M., Schoenberg, S., Weber, L., Wiegeleben, A., and Weissflog, W., 1983, *Wissenschaftl. Beitraege-Univ. Halle*, **41,** 18.
[28] Keller, P., Cladis, P. E., Finn, P. L., and Brand, H. R., 1985, *J. Physique*, **46,** 2203.
[29] Wiegeleben, A., Richter, L., Deresch, L., and Demus, D., 1980, *Mol. Cryst. liq. Cryst.*, **59,** 329.
[30] Goodby, J. W., Gray, G. W., Leadbetter, A. J., and Mazid, M. A., 1980, *J. Phys. (Paris)*, **41,** 591.
[31] Shashidar, R., Kalkura, A. N., and Chandrasekhar, S., 1980, *Mol. Cryst. liq. Cryst.*, **64,** 101.
[32] Klose, G., Grande, S., Franck, U., Grossmann, S., and Moebius, G., 1987, *Mol. Cryst. liq. Cryst.*, **150B,** 201.
[33] Barbera, J., Melenez, E., Serrano, J. L., and Sierra, M. T., 1988, *Ferroelectrics*, **85,** 405.
[34] Stoebe, T., Geer, R., Huang, C. C., and Goodby, J. W., 1992, *Phys. Rev. Lett.*, **69,** 2090.
[35] Geer, R., Stoebe, T., and Huang, C. C., 1993, *Phys. Rev. E*, **48,** 408.
[36] Jin, A. J., Stoebe, T., and Huang, C. C., 1994, *Phys. Rev. E*, **49,** 4791.
[37] Jin, A. J., Veum, M., Stoebe, T., Ho, J. T., Hui, S. W., Surendranath, V., and Huang, C. C., 1996, *Phys. Rev. E*, **53,** 3639.
[38] Schlauf, D., Bahr, C., Glogarova, M., Kaspar, M., and Hamplova, V., 1999, *Phys. Rev. E*, 6188.